JOURNAL OF PROPULSION AND POWER
Vol. 12, No. 6, November–December 1996

Arcjet Modeling: Status and Prospects

Manuel Martinez-Sanchez*
Massachusetts Institute of Technology, Cambridge, Massachusetts 02139-4307
and
Scott A. Miller†
The Aerospace Corporation, Los Angeles, California 90009-2957

The evolution of arcjet thruster modeling to its current state of development is traced, and the most pressing theoretical uncertainties in the way of further progress are discussed. The thrust-producing mechanism is well understood, and so is the general energy balance, leading to voltage prediction, provided anodic attachment is separately known. This particular problem is discussed in some detail. It is argued that three-dimensional arc root constriction is a very likely cause of at least some of the observed anode behavior, and should be theoretically investigated. Other issues examined are electron–molecule interactions, species segregation, and thermomechanical effects.

Nomenclature

A, A_a	= cross-sectional area, arc cross-sectional area
c^*	= characteristic speed
$\bar{c}_e$	= thermal mean speed of electrons
c_F	= thrust coefficient
E	= electric field
e	= electron charge
F	= thrust
j	= current density
K	= thermal conductivity
k	= Boltzmann's constant
$\dot{m}$	= mass flow rate
m_e, m_i, m_g	= electron mass, ion mass, gas molecule mass
n_e, N	= electron number density
p, P	= pressure
Q	= collision cross section
R, R_a	= radius of constrictor or nozzle, radius of arc
R_g	= gas constant
T, T_e, T_g	= temperature, electron temperature, gas temperature
u	= electron energy
ΔV_a, ΔV_c	= anode and cathode voltage drops
δ	= inelastic loss factor, Eq. (7)
ρ	= mass density
σ	= electrical conductivity
v_B	= Bohm velocity

Introduction

LIKE many other practical devices, arcjets for space propulsion have evolved largely on the basis of a series of intuition-guided empirical developments, with theory providing at best a general background, and very little detailed help to the designer. While scientific data and submodels have existed for a long time regarding the properties of arcs, in general, the interactions of arcs with strong flowfields introduce so much additional complexity, that until recently, there was little hope of being able to construct comprehensive models of the complete device. The situation is now rapidly changing because of the combination of greatly expanded computational resources, and renewed interest in refining arcjets for a variety of operational space uses. In synergy with these facts, new physical information is also being generated via a new generation of plasma diagnostics. The net result is an exciting rapid increase of our understanding of arcjets. Theory still lags substantially behind practice, but the gap seems now bridgeable for the first time.

In this article we will provide a synoptic summary of the controlling physics, review the arcjet modeling literature, and examine in more detail some of the more difficult mechanisms at work. We will conclude with a look ahead and a prognosis for the near future in this field.

Received Nov. 2, 1994; revision received March 8, 1996; accepted for publication April 10, 1996.

*Professor, 77 Massachusetts Avenue, 37-401.
†Senior Member of the Technical Staff, M4-969, P.O. Box 92957.

Essential Arcjet Physics

After initial experimentation with other arrangements, arcjet design has settled to the basic configuration illustrated in Fig. 1, in which an arc burns coaxially with the flow, ahead of the supersonic part of the nozzle, although a variation in which the arc attaches ahead of the sonic point has also been developed.[1,2] In either case, a prominent feature of the arcjet flowfield is the existence of an intensely heated, hence, low density, core as the flow passes the sonic section. Because of this heterogeneity, and also because of the extreme specific enthalpy levels achieved in parts of the flow, the detailed physics of the arcjet is quite complicated. In this section we attempt to identify those among the many competing effects that matter the most for performance prediction, and which must be captured by all successful models.

Prediction of Thrust and Specific Impulse

As previously noted, very little mass is carried inside the arc; in essence, the arc acts as a fluid-dynamic partial plug on the flow, so that, if A_a is the arc cross section suitably defined and A is the constrictor cross section, the flow-carrying area is $A - A_a$. The flow chokes at (or near) the constrictor exit,

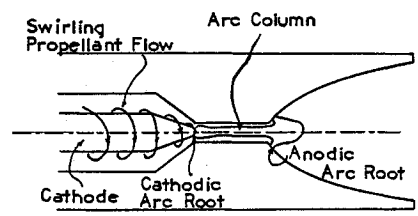

Fig. 1 Basic configuration of an arcjet with supersonic arc attachment.

where this area is least, and, if $P_{0,out}$ and $T_{0,out}$ are the outer flow stagnation pressure and temperature

$$\dot{m} = \frac{P_{0,out}(A - A_a)}{c^*_{out}} \tag{1}$$

with c^*_{out} being the familiar characteristic speed of a rocket chamber, proportional to $\sqrt{R_g T_{0,out}}$ (R_g being the gas constant). On the other hand, the also familiar mechanical interpretation of a rocket's thrust states that this thrust arises from the lack of a reaction surface for $P_{0,out}$ in the area of the throat (times a nozzle coefficient c_F of order 1–2, accounting principally for the pressure forces on the diverging nozzle bell):

$$F = c_F P_{0,out} A \tag{2}$$

Notice that the whole constrictor area A is used, because P is constant across it. Aside from some incidental change in c_F caused by peculiarities of the arcjet flow, Eq. (2) is as it would be in the absence of the arc, but Eq. (1) is very different. The specific impulse I_{sp} is given by

$$gI_{sp} = F/\dot{m} = (c_F c^*_{out})[A/(A - A_a)] \tag{3}$$

where the factor in parentheses would be obtained with no arc.

Equation (3) shows the crucial elements for successful specific impulse prediction:

1) The stagnation temperature of the outer gas needs to be well predicted. In an operational sense, this highlights the importance of regenerative cooling, or of any steps taken to raise the temperature of the outer gas (this may not necessarily imply raising the anode wall temperature, because the thermal boundary layer is comparatively thin).

2) The size of the arc at the constrictor exit needs to be accurately predicted. Since the arc growth is a result of radial diffusion of ohmic heat into the coflowing outer gas, the implication is that the thermal diffusivity and the electrical conductivity must be modeled accurately. This may not require, however, more than a parametric transport property representation, which is faithful over a broad temperature range, even if some level of detail needs to be sacrificed.

Operationally, the factor $A/(A - A_a)$ in Eq. (3) implies that the constrictor length and diameter should be designed such that the arc comes as close as thermally allowable to the constrictor wall. Since different gases and different operating points lead to different arc radii, this fact needs to be also taken into account. For example, the speed of sound in N_2 is about one-quarter that in H_2 at the same temperature, giving the arc four times longer growth time in a given constrictor length when running in N_2. There is also some difference in heat diffusivity but, to a first order, a satisfactory constrictor for H_2 will lead to premature attachment if run in N_2, as noted in Ref. 3.

Other factors affecting thrust prediction include the actual velocity profile in the arc periphery and the effects of wall friction. As an example of the latter, consider the constrictor H_2 flow in the 20-kW arcjet of Ref. 3. The Reynolds number based on its 5 mm length is $\sim 10^4$, giving a total laminar boundary-layer thickness of about 0.17 mm (corroborated by the computations of Refs. 4 and 5) and a net viscous drag of 0.016 N. There is additional drag in the nozzle, but its magnitude per unit length ($\pi\rho u^2 R c_f$) decreases rapidly, so that the net viscous drag is of the order of 0.05 N, compared to thrust levels in the 0.5–1.5 N. The relative effect will be somewhat larger at smaller powers [roughly as $(\text{Power})^{-1/4}$]. The message here is that, while important because of the low Reynolds numbers involved, arcjet viscous thrust losses remain secondary.

As interesting as what is essential for thrust prediction, is what is not. In particular, Eqs. (2) and (3) show that the conditions inside the arc itself (dissociation, ionization, nonequilibrium, etc.) are fairly irrelevant in this regard, as long as the arc radius can be calculated. This partly accounts for the success of many simple models in thrust and specific impulse predictions.

Prediction of Voltage

For a fixed current, voltage determines the power absorbed by the arc, and its calculation, involving as it does an accounting of energy losses, is generally more difficult than that of the thrust.

The voltage is naturally divided into the column voltage and the electrode drops. The main difficulty with column voltage is the determination of column length, i.e., the location of the anodic arc attachment. If the length is separately known, the field $E = dV/dx$ is no more difficult to calculate than the arc radius R_a. This follows from the radial energy balance

$$\pi R_a^2 \bar{\sigma} E^2 \cong [\bar{K}(T_c - T_e)/R_a] 2\pi R_a \tag{4}$$

or, using $\bar{\sigma} \approx \frac{1}{2}\sigma_c$, with c referring to the arc centerline,

$$E \cong 2\frac{\sqrt{\bar{K}(T_c - T_e)/\sigma_c}}{R_a} \tag{5}$$

which shows an inverse dependence of the arc voltage on the constrictor radius.

The phenomena in the cathode spot area are too complex for the level of modeling likely to be of interest for propulsion, and their performance impact is summarized by one insensitive quantity, namely, ΔV_c, for which empirical information does exist.[6,8] A separate issue relates to cathode lifetime, which has so far largely defied modeling, because, in addition to mass loss, one would also need to deal with morphology changes (e.g., whisker growth), which tend to be the life-limiting factors in arcjet applications.

Accurate prediction of the anode fall ΔV_a is probably bound up with the issue of attachment determination. On the other hand, the magnitude of ΔV_a is becoming more amenable to first-principles calculations. Two components of ΔV_a can be discerned:

1) A resistive drop occurring in the electron-deficient (but still quasineutral and collisional) layer adjacent to the anode. This layer is thin (~0.1 mm) and is determined by the balance of ambipolar losses to the wall and excess ionization sustained by the enhanced radial field. The computations of Miller[4,5,7] have been able to resolve this sublayer in the context of a

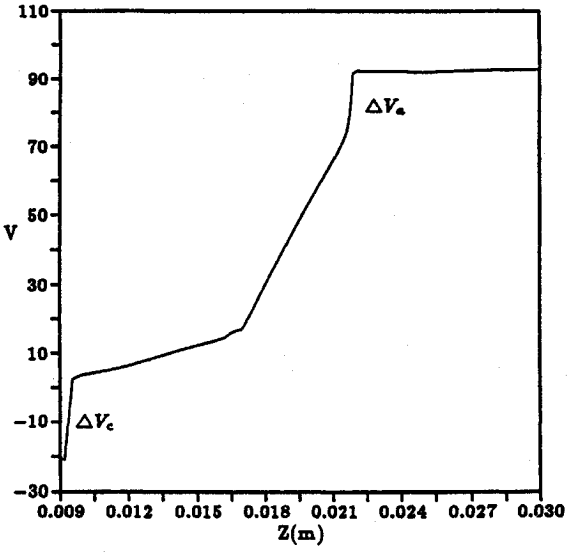

Fig. 2 Electric potential axial profile for the baseline case arcjet simulation.[8]

whole-thruster simulation. Figure 2, from Ref. 7, shows a profile of voltage from the cathode, along the arc axis and across the anodic bridge to the anode surface. The rapid, but resolved, voltage increase near the anode surface can be noted.

2) A sheath voltage drop, typically negative (anode below local plasma potential), which is required to turn back the excess thermal flux of electrons beyond those required by the circuit. This contribution is $\Delta V_{a,s} < 0$, given by

$$j = en_e[(\bar{c}_e/4)\exp(e\Delta V_{a,s}/kT_e) - 0.61v_B] \quad (6)$$

where $v_B = \sqrt{kT_e/m_i}$ is the Bohm velocity, with which ions enter the ion-attracting sheath. Here, j is the local current density at the anode surface, which needs to be self-consistently computed at the same time.

The preceding description of the anode is not incompatible with the possibility of three-dimensional constriction, discussed later, but actual resolution in a three-dimensional computation is still beyond reach.

In summary, adequate calculations of voltage, and, hence, efficiency, are becoming possible, although many models are still incapable of direct determination of anode drops. This, plus uncertainties in cathode and column voltages, typically yields a scatter of $\pm 20-40$ V in reported results.

Prediction of Heat Losses

This is important from the thruster integration point of view, in addition to its direct effect on efficiency. The dominant contributor to wall heat flux is simply the product of anode drop times current, with ordinary conduction/convection playing a secondary role. While this somewhat facilitates the performance modeling task, it also means that an accurate prediction of the heat flux distribution, and, hence, of the peak wall temperature, depends critically on being able to calculate the current distribution at the anode, which, as we have seen, is still somewhat elusive. Once the wall flux is determined, it is a relatively simple task to calculate the temperatures throughout the anode block, accounting for either radiation or regenerative cooling. One caveat in this respect is that the wall thermal reaction time (a few seconds) is orders of magnitude longer than the flow reaction time (tens of microseconds), so that a fully coupled computation is impractical. Fortunately, the detailed wall temperature distribution has only a minor effect on both performance and current distribution in the plasma (as long as the gas temperature is nearly correct). It appears that one or two cycles of iteration on the wall temperature, starting from a reasonable guess, are sufficient for convergence.

Literature Review

We next illustrate the main lines of development of thermal arcjets modeling in the past. Although related, we will omit discussion of work on the so-called magnetoplasmadynamic (MPD) arcjets. Also, because of space limitations, we will not include here any discussion of plume flow modeling, an area that has seen significant recent developments. Many other less justifiable omissions will also undoubtedly occur, for which the author apologizes in advance.

Zero-Dimension Models

As discussed by Pfender[8] in his excellent review on arcs and arc heaters, the idea of using an electric arc for propulsion purposes grew out of the previous experience with arc gas heaters for chemical processing and other industrial uses. In an industrial arc heater the object is a uniformly heated gas exhaust, and devices such as magnetic arc rotators have been used to homogenize the temperature in a gas plenum. Drawing on this analogy, early electrothermal rocket models[9] evaluated frozen losses (mainly dissociation and ionization energy) by postulating uniform conditions in the heating chamber, from which the gas was assumed to then flow through a nozzle under isentropic (frozen, or, for reference, chemically equilibrated) conditions. When applied to arcjets, this procedure is fundamentally flawed because of the combination of the strong segregation of hot and cool gas in an arc and the very nonlinear variation of dissociation and ionization with temperature. Essentially, the frozen losses are confined to the arc itself, which may occupy a sizeable geometrical fraction of the arcjet throat, but carries only a minor part of the exhaust flow rate. Nevertheless, calculations based on such models did call attention to the large losses associated with frozen chemistry, and provided at least a qualitative explanation for the loss of efficiency at very high specific impulses.

Quasi-One-Dimensional Models

After the initiation of experimental work with constricted arcjets of the type still in use, the essential nonuniformity of the flowfield was recognized and accounted for in models. For example, John et al.[10] subdivided the flow into a core, a transition zone, and an outer region, and constructed a simple analytical model as a vehicle for interpreting test results of their 30-kW arcjet. This work identified the basic energy addition and loss mechanisms, including friction, chemical reaction, area ratio effects, etc. Similar work during the 1960s and 1970s was reported, for instance, by Weber[11] and Topham,[12] and more recently, by Glocker et al.,[13,14] Schrade and Sleziona,[15] Martinez-Sanchez and Sakamoto,[16] and Tahara et al.[17] This last mentioned model has been recently extended[18] to include an elaborate model of the nonequilibrium chemistry in a molecular gas arcjet.

The persistence of this type of quasi-one-dimensional modeling, despite the increasing availability of an array of more elaborate methods, is because of their recognized ability to mimic the most important aspects of arcjet operation and to provide reasonable performance estimates. In fact, if prediction of thrust and, to some extent, efficiency, were the only criteria by which models were to be chosen, there would be very little incentive for the vast increase in effort required at the next logical modeling level (two-dimensional models).

Two-Dimensional Models

One-dimensional models have serious limitations concerning the details of the gas physics and flow dynamics. While, with some operator skill, such models can come close to providing valid performance predictions, they offer little hope for design improvement based on exploitation of one or other of the many competing effects present. The inflexibility arises from the need to postulate simple gas physics to construct manageable integrated fluxes, whose evolution can then be traced with ordinary differential equations. Relaxing these constraints requires a detailed two- or three-dimensional description of the problem.

The initial work on two-dimensional (axisymmetric) arcjet modeling is from Watson and Pegot,[19] whose focus was the constrictor region alone. The gas was assumed to be in thermodynamic equilibrium, which is reasonable as long as the anodic attachment region and the nozzle are not examined. Viscous and heat conduction effects were included. The calculation was made by spatial marching, using what would now be called a parabolized Navier–Stokes approach. This work was seminal in clearly illustrating the interplay of ohmic heating and flow acceleration and in showing in detail the extreme nonuniformity of the flowfield. Efforts have been recently made[20] to supplement the Watson and Pegot model[19] with near-electrode and nozzle sections.

One of the first two-dimensional numerical arcjet models covering the complete thruster was that of Nishida et al.[21,22] This model ignored viscosity and heat conduction, and assumed one single temperature. Ionization kinetics was included, and the working gas was argon. The results showed current attachment upstream of the nozzle throat and no discernible constricted arc; this is, in fact, consistent with ex-

perimental results for argon, which tends to operate in this so-called low-voltage mode.[23,24] The neglect of thermal conductivity may, however, make this model inappropriate for the high-voltage mode, in which an arc spans the length of the constrictor and attaches downstream of it. This work was later extended to a full single-temperature Navier–Stokes formulation, allowing heat loss predictions, but leading to similar flow and current patterns. Fairly good thrust and efficiency predictions were obtained in comparison to experiment.

More relevant to practical arcjets operating in the high mode on molecular gases are the models of Refs. 25–30. Butler and King have developed a two-dimensional model that can deal with hydrogen, nitrogen or mixtures, and includes viscous and heat conduction effects, as well as chemical kinetics. Diffusion was absent originally,[25,26] but was added in Ref. 27. The electron and gas temperatures are assumed equal; the authors refer to this as a single fluid model, whereas others prefer to call it thermal equilibrium. The benefits of a two-temperature (two-fluid) approach were discussed in Ref. 26, but no results on this were reported. In the nondiffusive, single-temperature model of Butler and King, the electron density and the electrical conductivity are essentially zero outside the arc, and no simple mechanism exists for current to reach the anode. This is remedied by introducing a conductivity floor σ_0 of the order of 0.1–1 $(\Omega)^{-1}$/cm. The precise σ_0 is selected to provide a good prediction of total voltage, and its effect on calculated thrust is relatively minor (Fig. 3 from Ref. 26). Once the constant σ_0 is imposed, one loses the ability to predict the current distribution along the anode wall. More precisely, the model does calculate this distribution, but there is no feedback to the local σ_0 value; as we will see, this feedback leads to a certain amount of axial constriction, which is ignored here. Cappelli et al.[31] have compared the exit-plane predictions of this code to data for a 1-kW H_2 arcjet (the first such detailed flowfield comparisons attempted). Velocity is well predicted, but heavy-particle temperature is underpredicted significantly on the jet axis at the higher specific energies.

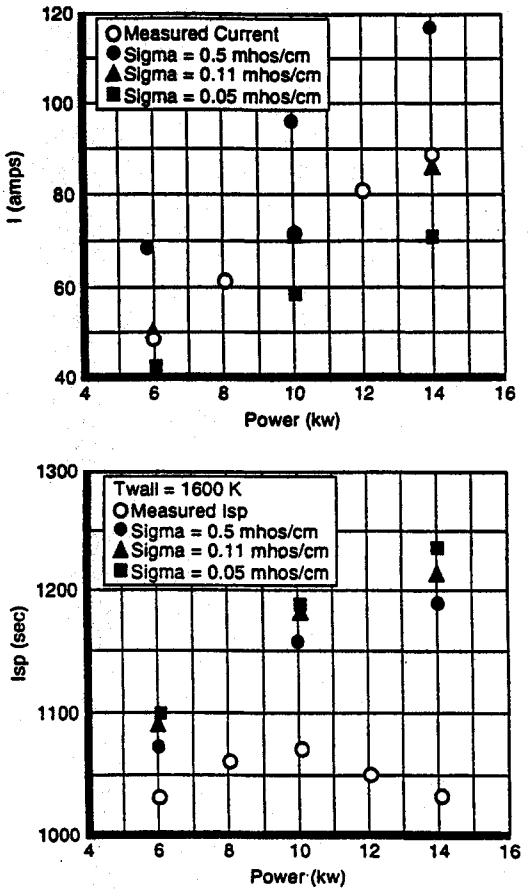

Fig. 3 Effects of conductivity floor.[26]

The addition of diffusion, particularly ion–electron ambipolar diffusion[27] has removed the need for the artificial conductivity floor, and somewhat improved the performance predictions. However, as will be seen, electron temperature elevation outside the arc column plays an even larger role than diffusion in bridging the gap to the anode wall.

The model of Rhodes and Keefer[28–30] also spans the whole arcjet, and incorporates full transport effect calculations for H_2 and N_2 and mixtures. Electron and gas temperatures are assumed equal in reported computations, although mention is made of incompletely converged two-temperature calculations, and chemical equilibrium is assumed throughout. The authors include radiation escape and radiation diffusion in the model. Radiation diffusion is the dominant thermal conductivity contribution in a narrow temperature range (≈12,000–14,000 K in H_2), where ionization generates significant free-bound transitions; it appears, however, that the overall significance of radiation is small, although it clearly dominates in related high-pressure, large-diameter arc heating applications. This point may require closer scrutiny. Once again, equilibrium forces a very low conductivity outside the arc, and an artificially elevated value is used for $T < 10{,}000$ K. The current distribution over the anode is specified a priori, which for a given voltage, results in excessive ohmic dissipation, requiring a correction factor of 0.75. Of course, the anode is not equipotential in general when current distribution is separately prescribed.

A comparable model, with a single temperature and Saha equilibrium, has been presented by Fujita and Arakawa.[24] Once again, an ad hoc remedy was necessary to generate sufficient near-anode conductivity, and it took the form of an ionization fraction minimum of 10^{-5}. The single-temperature assumption is probably even less adequate in this case, because argon was the test gas, and heavy monoatomic species couple very poorly to electrons in terms of energy.

The group working at the University of Pisa[32,33] has reported arcjet modeling work using single-temperature, equilibrium assumptions. Reference 32 focuses on the fluid mechanical effects of heat addition, whereas Ref. 33 provides comprehensive equilibrium chemistry and transport properties for hydrazine decomposition products under arcjet conditions.

The single-temperature assumption was abandoned by the authors of Refs. 4, 5, 7, and 34. Their model endows the electrons with a separate temperature ($T_e \neq T_g$, thermal nonequilibrium) and tracks the rates of ionization and recombination, rather than using ionization equilibrium at T_e. This requires a separate electron energy equation, which, aside from increasing the algebraic complexity, also requires special integration procedures because of its very short characteristic time. These authors[4,5,7,34] also included ion–electron ambipolar diffusion and finite molecular dissociation rates, plus a detailed calculation of molecular and electronic transport properties. As in other models, flow swirl is accounted for, although its role appears to be minor. Only hydrogen was modeled. The anode drop is modeled through Eq. (6) of this article.

The inclusion of thermal nonequilibrium and, to a smaller extent, ambipolar diffusion, enables the calculation of the current path outside the arc core, all the way to the anode wall. The essential point is the strong thermal nonequilibrium existing in what we could call the anodic bridge region, namely, the annular region connecting the arc at the constrictor exit to the initial part of the nozzle wall. This is illustrated in Fig. 4, which belongs to a simulation of the radiation-cooled 20-kW H_2 arcjet of Glocker et al.[3] In the arc core $T_e \cong T_g$, despite the very large ohmic power input to the electrons; this is because of the high degree of ionization, which ensures strong collisional coupling to the heavy particles. But outside the core n_e falls rapidly and this coupling is weakened to the point that T_e remains in the 10,000–20,000 K range, whereas T_g asymptotes to the outside gas temperature (~1000 K). This elevated T_e

makes it possible for the ionization rate to keep up with recombination and diffusive losses and to maintain an electron density $\sim 10^{20}$ m^{-3}, right up to the wall (Fig. 5). This represents an ionization fraction of only 10^{-4}, but is sufficient to provide the required electrical conductivity in this critical region. Miller's model[4,5,7,34] assumes insulating constrictor walls to force a downstream arc attachment. As will be discussed later, convection was found insufficient to drag the arc foot downstream, which points to the possibility of still unresolved physical effects at the anode root. The predictive accuracy of Miller's model is good (both for thrust and for voltage), although still comparable to what can be obtained using one-dimensional models, plus some empiricism.

Thermal nonequilibrium $T_e \neq T_g$ has also been incorporated in the more recent models by Fujita and Arakawa[35,36] and by Krier et al.[37] and Megli et al.[38] Fujita and Arakawa[35,36] first applied their nonequilibrium model to argon[35] (which operates in the low voltage, upstream attachment mode), and made a careful comparative study of the effects of ignoring all forms of nonequilibrium or, alternatively, ignoring electron temperature elevation while still accounting for chemical kinetics. Figure 6[35] shows clearly the relative effects of these various approximations; in general, ignoring the degrees of freedom allowed by nonequilibrium tends to delay arc attachment. The model with both thermal and chemical nonequilibrium yields close agreement with experiment.

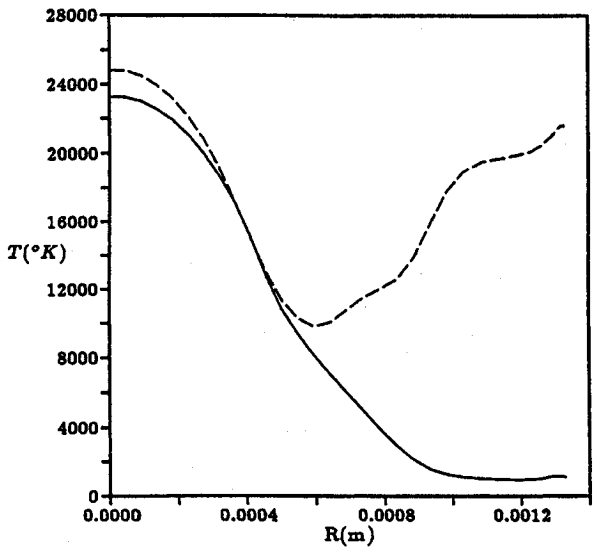

Fig. 4 Radial profiles of gas and electron temperature 0.25 mm downstream of the constrictor exit for the baseline case arcjet simulation (——, gas and – – –, electron temperatures).[34]

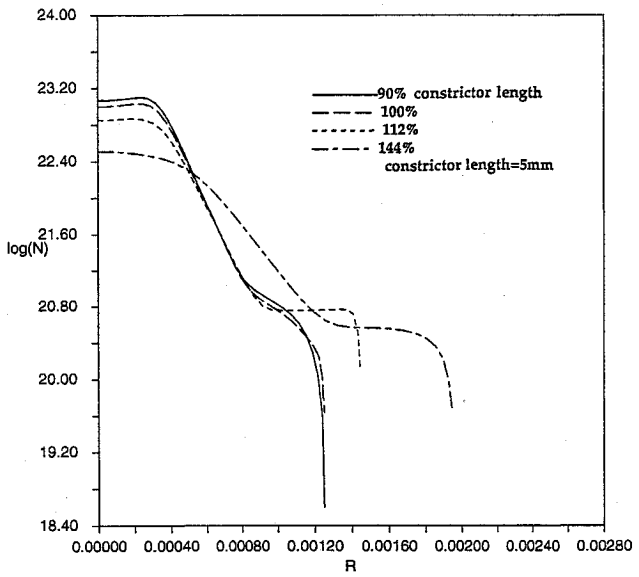

Fig. 5 Radial profiles of electron density for conditions of Ref. 5 ($\dot{m}$ = 0.1 g/s, I = 60 A), at several axial sections near the constrictor's end (N in m^{-3} in M).

In their later paper, Fujita and Arakawa[36] extended the model to hydrogen as well, and included simple models for the voltage drops at anode and cathode [the anode model is the same as that of Eq. (6), while the cathode model was partially bypassed by using an assumed cathode temperature]. The calculated electron and heavy particle temperatures were similar in magnitude and distribution to those found by Miller.[4,5,7,34] Thus, Fujita's results[36] for the ARTUS 1.5-kW H_2 arcjet at a specific energy of 1.29×10^8 J/kg yielded a centerline temperature (both T_e and T_g) of 23,000 K at constrictor exit, while Miller's results[34] for the same location and specific energy gave $T_e \cong T_g \cong 25{,}000$ K. In both cases, T_e and T_g diverged outside the arc, as in Fig. 4.

Unlike Miller,[34] however, Fujita and Arakawa[36] allowed a fully equipotential anode, including the constrictor. This had the effect of redistributing a fraction of the current to the upstream area, although most of it still attached downstream. This important difference between what appears to be very similar models, is at this time unexplained. Perhaps because of the partial upstream attachment, Fujita and Arakawa's predicted voltage[36] was consistently low by about 15 V compared to data, and the specific impulse was consistently high by $\approx$100 s.

Krier et al.[37] described their two-temperature formulation (which they call kinetic nonequilibrium, a term others reserve for finite chemical rates) and reported significant results for H_2 and N_2–H_2 mixtures.[38] By comparing simulations with chemical equilibrium (CE) and finite rates (CNE), they again confirmed the general conclusion that nonequilibrium leads to an upstream shift of the attachment, as well as other flow features. The electron and gas temperature profiles resemble those of Miller[34] and Fujita and Arakawa[36] ($T_e \cong T_g$ in the core, $T_e >> T_g$ outside core), but are generally lower, more in line with observations.[39,40] With N_2 present, the T_e calculation using the low δ, as given in Ref. 41, appeared to allow excessive electron temperatures outside the arc, and led to voltage underpredictions by 30–40 V and to upstream attachment. Using the much higher δ inferred from Nigham's work[42] by this author (see following section) restored agreement and also forced the arc to attach downstream. This result gives one further clue regarding attachment: it is possible that a similar problem occurred in Miller's hydrogen model,[34] which also used accepted δ values from Ref. 41.

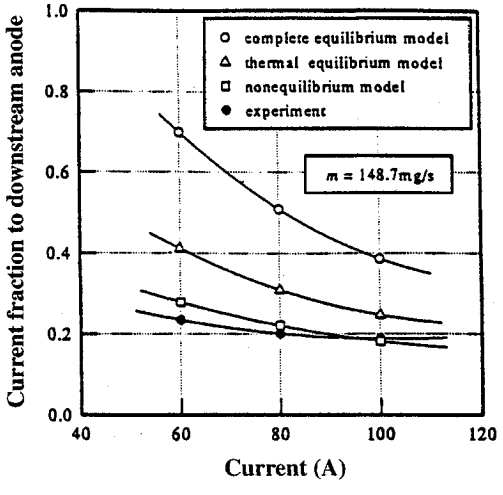

Fig. 6 Current distribution in terms of current fraction to downstream anode ($\dot{m}$ = 148.7 mg/s).[35]

Modeling Challenges

Despite all of the progress, our confidence in first-principles arcjet models is not yet sufficient to allow their routine use for design, particularly if this involves deviations (such as subsonic attachment or seed addition) from familiar configurations. The reason is that there remain several basic effects that are poorly understood, and others where the basic scientific data exist, but have yet to be incorporated in our models. This section will briefly review the most salient of these issues.

Near-Anode Region

As was pointed out in the Literature Review, we have progressed here from artificial ionization or conductivity floors through electron diffusion and, more recently, electron overheating, as mechanisms to provide conduction to the anode wall. While this appears to have resolved this issue for argon,[35] the difficulties still encountered for H_2 (Ref. 34) and N_2 (Ref. 38) suggest that more needs to be learned about electron-heavy gas coupling in this region. The freedom allowed for T_e to rise above T_g, which is essential to establish an ionized bridge between arc core and anode wall, may have been excessive in some of the models. In the fully decoupled limit, which Miller's H_2 model[7,34] approaches, the bridge is sustained by hot electrons, with no disturbance to the crossflowing heavy gas; there is then no obvious effect capable of convecting this electronic bridge downstream, and one is left with counterflow electronic heat diffusion, which tends to move the arc attachment upstream. The opposite limit is, of course, the modeling assumption of thermal equilibrium ($T_e = T_g$ throughout); this is known to either forbid attachment anywhere (unless aided by a minimum conductivity), or, at best (particularly when diffusion is included), to lead to excessive downstream convection of the attachment point.

At least two avenues appear possible that would lead to a stronger *e*-gas coupling without resorting to overall thermal equilibrium: 1) three-dimensional constriction and 2) increased inelastic electron energy losses. These will be further explored later.

Azimuthal Nonuniformity and Nondiffuse Attachment

Closely allied with the attachment problem is the issue of whether the axial symmetry assumption is valid. It is conceivable that the arc bridge might become three-dimensionally constricted at some point, resulting in attachment via spokes (which would rotate because of the flow swirl). In that case, the much higher local plasma density in the spoke would indeed elevate T_g (as in the arc core itself, see Fig. 4) to near T_e, and the attachment physics would radically change. In particular, models such as those of Maecker[43] and its follow-on by Yamada et al.,[44] now become relevant. Maecker[43] argues that an arc moves by a superposition of mass motion of the heated gas and motion of the high-temperature zone with respect to the gas. In a steady arc in crossflow, such as the anodic bridge, these contributions add up to zero velocity. Maecker[43] proceeds to relate the local curvature of the arc to the crossflow velocity (as in a horizontal arc subject to upwards convective flow), and Yamada et al.[44] extend the model to calculate the point of attachment to a cylindrical anode. Aside from the relative crudity of some of the assumptions made (e.g., the crossflow speed in the arc core is set equal to the external normal speed, times the inverse density ratio, as if the flow direction remained undisturbed), one needs to keep in mind that the basic Maecker's model[43] is based on a bent core, with high gas temperature. Three-dimensional constriction appears necessary for this.

The problem of the stability of the axisymmetric solution remains largely unexplored. Miller[7] performed some linearized electrothermal stability analysis, assuming only planar disturbances with an axial wave vector. Although the axisymmetric stability problem would involve tangential wave vectors, the difference may be small, because, as noted, convective effects play a minor role in the basic solution. The results indicated stability for the conditions of the numerical studies, but they also showed that instability would result at higher current densities and lower ionization fractions; given the inaccuracies in the stability model (uniform background and undisturbed heavy species), the potential for constriction cannot be dismissed. Figure 7, for example, maps the stability region as a function of normal current density. Modes with wave number $k_\perp \leq 5000$ m^{-1} ($\lambda \geq 1$ mm) can become unstable when $T_e \sim$ 25,000 K, if the basic currents density exceeds 10^7 A/m^2; the approximate peak current density in the baseline case (0.1 g/s, 100 A) was 3×10^6 A/m^2.

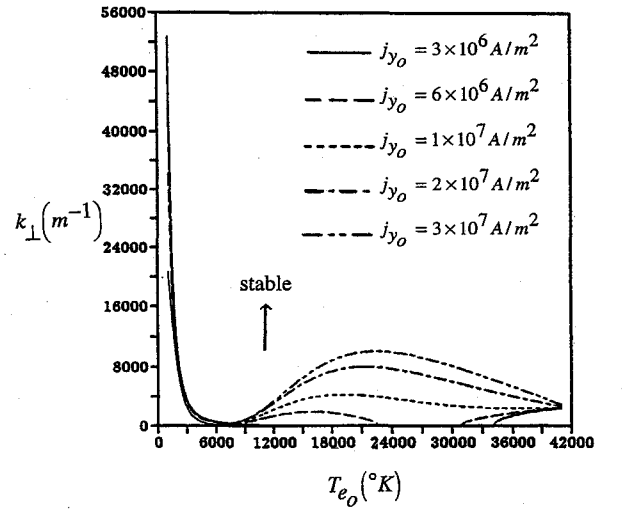

Fig. 7 Neutral stability lines as a function of the zeroth-order electron temperature and current density with nonequilibrium ionization.[7]

More refined stability studies of the attachment region are desirable, given the important implications of constriction. These studies are analytically challenging, and, with steady progress in the numerical area, perhaps a direct three-dimensional numerical attack is a near-term possibility. An interesting intermediate course would involve numerical solution of a linearized three-dimensional model, starting from a converged two-dimensional simulation, although any linear analysis will miss the constricted end state, which can only be captured by a full three-dimensional simulation.

Some experimental evidence of three-dimensional constriction in the attachment area has been reported by Harris et al.,[45] who tested a radially segment arcjet and observed a generally nonsymmetric distribution of current to the segments, with random fluctuations, indicative of a multifilament structure of the anodic bridge.

Similar experiments, but with axial segmentation of the attachment region, were performed by Berns et al.[2] In this case, the attachment was confined to an extended cylindrical region upstream of the nozzle throat, as in the older Giannini arcjet design,[1] with arc stabilization being provided mainly by the flow swirl. Berns et al.[2] observed oscillations in the segment currents and overall voltage, which indicated downstream convection of the attachment point until a new restrike occurred near the cathode, presumably when the local arc-to-anode voltage in that region exceeded some threshold. This same restrike behavior had also been mentioned by Pfender[8] as being common in plasma torches. In Berns et al.,[2] when the arc foot passed through the throat to the supersonic region of the nozzle, the operation tended to be restrike free, but the incidence or absence of restrike is not well documented[46] for the usual supersonic attachment designs. In any case, their occurrence in the subsonic attachment case appears to lend support to the view that the anodic bridge may be constricted in a three-dimensional sense, because, as noted, this should then lead to its convection by the flow.

Molecular and Molecule-Induced Nonequilibrium

A different area where modeling needs improvement is that of nonequilibrium molecular effects. These include slow kinetics or freezing of vibrational and rotational modes in the nozzle expansion (certainly in the plume), as well as distortion of the electron energy distribution associated with strong cross sections for inelastic electron–molecule collisions.

Of these two issues, the first is probably the least significant, although uncertainties remain. Zube and Myers[47] were able to measure electronic excitation temperature, as well as rotational and vibrational temperature, in a 1-kW H_2–N_2 arcjet, at several points in the supersonic nozzle. They found that the excitation temperatures remained above 10,000 K at the nozzle exit, but the apparent indication of a very high exit plane T_e was dispelled by a more refined analysis by Zube and Auweter-Kurtz,[48] using a method by Park[49] to correct for lack of Boltzmann equilibrium among electronic states. The true T_e was found to be 3000–4000 K, in agreement with model results by Miller[7] and with measurements by Hoskins et al.[50] More important for the present discussion, the vibrational temperature was found in Ref. 47 to track closely the rotational temperature during the nozzle expansion, both of them decaying to 2500 – 3000 K at the exit plane. In contrast, in a 5–10-kW N_2 arcjet study, Tahara et al.[17] observed that the rotational temperature, after an initial drop from an already high 9000–6000 K, subsequently rose in the nozzle to an exit plane value of 7000–10,000 K. The latter tests were at fairly low pressure (a 6-mm-diam constrictor was used, giving chamber pressures of 0.1–0.3 atm), which may explain the anomalous behavior.

In terms of modeling, accounting for vibrational lag is relatively straightforward (for example, as in Ref. 51), although it does involve additional computational burden. A more comprehensive approach, in which the state-specific vibrational populations are tracked separately,[52–54] is, by contrast, quite demanding in the context of a two-dimensional computation, and, in view of the data, would not seem justified for the normal operational regimes. It may, however, be needed to understand the effects on the free electron distribution, to which we now turn.

It is well known that molecular gases, particularly N_2, can readily absorb collisional energy from the free electrons into their vibrational modes. For N_2, this occurs mainly for electron energies from 2 to 3 eV. As a result, for values of the field/density E/N ratio high enough that significant population of electrons would exist above these energy levels in atomic gases, very few may actually exist in a molecular gas if its vibrational population temperature is significantly lower than T_e. The electon distribution dams up against the effective barrier represented by the vibrationally active region of the energy spectrum, and it greatly departs from the Maxwellian shape. Typical results by Nighan[42] are shown in Fig. 8. For reference, Fig. 9 shows calculated E/N in the anodic bridge region of an H_2 arcjet, using the model of Refs. 4 and 5.

For N_2, if $E/N \leq 5 \times 10^{16}$ V cm^2, there develops a substantial depletion of high energy electrons. If this persists all the way to the ionizing range (13–16 eV), the ionization rate calculation would be substantially affected. In this connection, it must be noted that for each E/N, the results of Nighan[42] appear to indicate that the distribution actually becomes super-Maxwellian at high enough electron energy; however, the reported range of $f(u)$ (Fig. 8) is insufficient to verify where this happens for the lower E/N values. Other electron-induced rates, such as vibrational excitation and dissociation, must be also strongly affected by the distortion in $f(u)$.

The traditional way to account for vibrational (more generally, inelastic) losses in molecular gases is to multiply the elastic losses times a factor δ, which is energy dependent. Data on these factors were collected by Massey and Craggs[55] and are reported in Ref. 41. Equation (5.74) of Ref. 41 gives the electron temperature elevation as

$$\frac{T_e}{T_g} = 1 + \frac{\pi}{24\delta}\frac{T_g}{T_e}\frac{m_g}{m_e}\frac{e^2}{Q_{eg}(T_e)}\left(\frac{E}{P}\right)^2 \qquad (7)$$

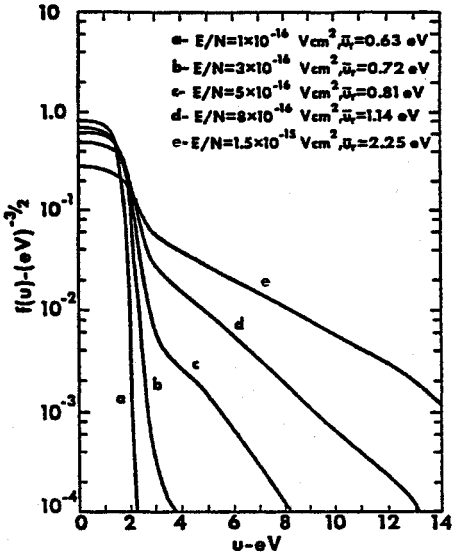

Fig. 8 Electron energy distribution functions in N_2 for various E/N values. The distribution function is defined such that $\int_0^\infty u^{1/2} f(u)\, du = 1$, and the reduced average energy such that $\bar{u} = \frac{2}{3}\int_0^\infty u^{3/2} f(u)\, du$.[42]

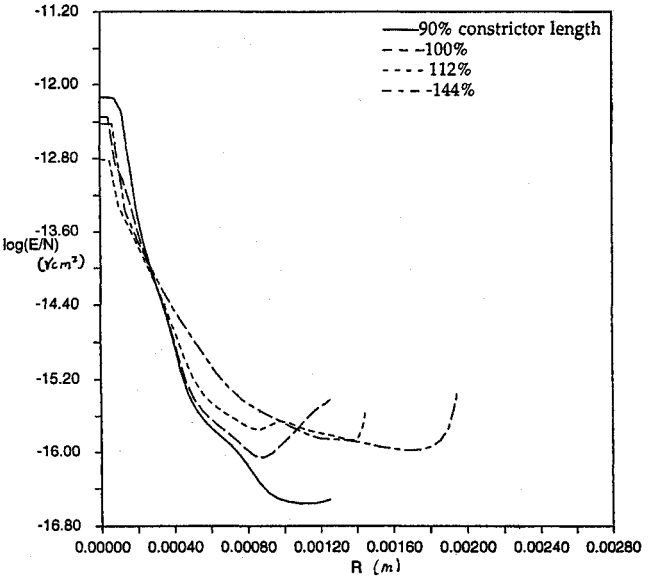

Fig. 9 Radial profiles of E/N (V cm^2) for conditions of Ref. 5 (0.1 g/s, 60 A) at several axial sections near the constrictor's end.

We can use the Nigham results[42] in Fig. (8) and Eq. (7) (where $P = NkT_g$), to extract the effective δ value implied. We do this by equating T_e to the mean energy $\bar{u}$, in Fig. 8 and using known data for the elastic cross-section $Q_{eg}(T_e)$ (Ref. 56). The value of T_g needs to be assumed, and 0.1 eV has been used here. The resulting δ is shown superimposed on the Massey–Craggs data[55] in Fig. 10, and a very large discrepancy is readily appreciated. With Nighan's results,[42] if $E/N \sim 10^{-16}$ V cm^2, as in the anodic bridge region, then $T_e \sim 0.6$ eV, and a very non-Maxwellian distribution results, whereas using, as in Refs. 4, 5, and 34, the Massey-Craggs data,[55] we found $T_e \sim 1$–2 eV, which, back to Fig. 8, would indicate little departure from Maxwellian.

In view of the uncertainties, and of the strong potential implications, there is clearly a need for more detailed research in this particular area. Babu and Subramaniam[53] have initiated work in that direction.

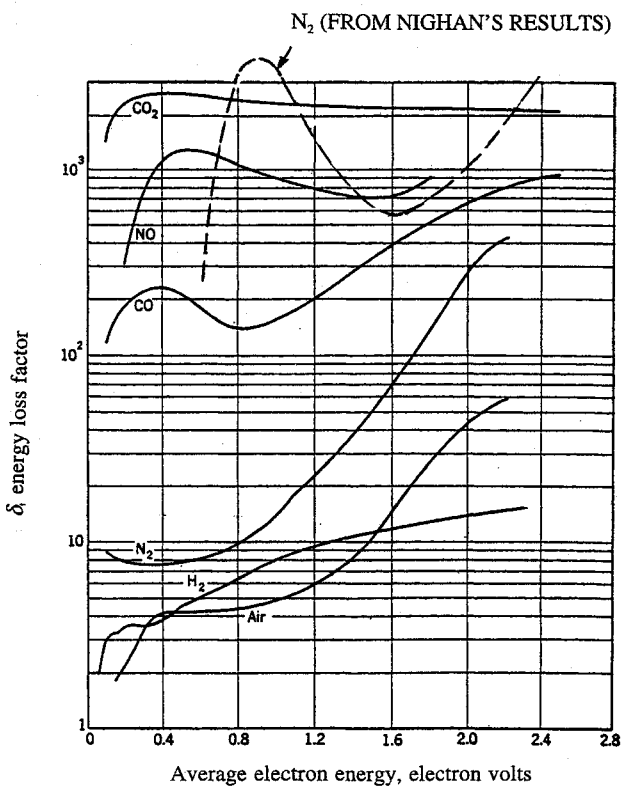

Fig. 10 Energy loss of electrons with Maxwellian velocity distribution with various gases.[55] Superimposed are calculations on δ based on results in Fig. 8 for N_2.

Thermomechanical Effects

A knowledge of the anode wall temperature distribution is required for an accurate prediction of performance, especially concerning its effect on the temperature of the cooler buffer gas, which controls flow and thrust. This is apparent in the performance variations observed during the warm-up period. There could also be a direct effect of wall temperature distribution on arc anodic attachment, although this point is less well established (computations by Miller[6,8] showed only small effects). Many of the two-dimensional codes referred to in the Review section have incorporated a thermal model of the anode block as well, the only difficulty being the very long thermal response time ($\approx$1 s), which requires iteration of the gas flow calculations with the wall temperature distribution kept frozen between iterations, and updated from the computed gas-side heat fluxes.

On the other hand, the materials comprising the anode block structure of an arcjet are subject to extreme heat fluxes (1–10 $\times$ 10^7 W/m^2 in the attachment area) and reach temperatures that can be over one-half of their melting point. Thus, despite a low stress level, thermal creep effects can occur, which distort the critical constrictor region, as has been observed, for example, by Butler,[57] and lead to performance drift and lack of repeatability, and may also affect thruster life. Related effects can occur in cathodes at high current.[58] From the modeling point of view, these areas remain unexplored, and, given their practical importance, efforts should be made to extract as much related information as possible from heat flow models of the solid part of thrusters.

Species Segregation and Mean Free Path Effects

In an arcjet using N_2H_4 or NH_3, these heavy molecules will dissociate as they enter the arc-heated parts of the flow. The hydrogenic fragments resulting from this dissociation will diffuse much faster than the nitrogen molecules or atoms, and the result can be a hydrogen enrichment of the cooler, outer parts of the flow.

A similar segregation of hydrogen toward the periphery is also to be expected in the plume after collisionality has become very weak, simply because of the higher thermal velocity of H and H_2 compared to N and N_2 (or NH) at the same temperature.

These two effects are observed together when looking spectroscopically at the arcjet plume, yet their implications are quite distinct (segregation upstream can improve specific impulse, segregation in the plume cannot). Refined diffusional and/or Monte Carlo computations will be required to mimic these effects.

Summary

Numerical modeling of arcjet thrusters is reaching an acceptable level of performance prediction capacity, predicated, however, on a judicious admixing of empirical information on a number of poorly understood physical issues. Prominent among these are the physics of anodic attachment (including stability and potential filamentation), and the interactions of free electrons with the molecular gas. Further progress will necessarily have to include clarification of these areas, plus gradual expansion of the ability to handle the very complex numerical task while staying financially solvent. The time appears at hand when theoretical modeling can emerge from the shadow of empiricism and become a routine tool, together with selective testing in the quest for improved design of future thrusters.

Acknowledgments

This work was made possible under the support of the U.S. Air Force Office of Scientific Research Grant 91-256. The Technical Monitor was Mitat Birkan.

References

[1]Todd, J. P., and Sheets, R. E., "Development of a Regeneratively Cooled 30 KW Arcjet Engine," *AIAA Journal*, Vol. 3, No. 1, 1965, pp. 122–126.

[2]Berns, D., Sankovic, J., and Sarmiento, C., "Investigation of a Subsonic-Arc-Attachment Thruster Using Segmented Anodes," AIAA Paper 93-1899, June 1993.

[3]Glocker, B., Auweter-Kurtz, M., Goez, T. M., Kurtz, H. L., and Schrade, H. O., "Medium Power Arcjet Thruster Experiments," AIAA Paper 90-2531, July 1990.

[4]Miller, S. A., and Martinez-Sanchez, M., "Multifluid, Non-Equilibrium Simulation of Arcjet Thrusters," AIAA Paper 93-2101, June 1993.

[5]Miller, S. A., and Martinez-Sanchez, M., "Nonequilibrium Numerical Simulation of Radiation-Cooled Arcjet Thrusters," *Proceedings of the 23rd International Electric Propulsion Conference* (Seattle, WA), 1993 (Paper 93-219).

[6]Guile, A. E., "Arc Electrode Phenomena," *IEEE Reviews*, Vol. 118, No. 9R, London, 1971, pp. 1131–1154; also "Basic Erosion Processes of Oxidized and Clean Metal Cathodes by Electrical Arcs," *IEEE Transactions on Plasma Science*, Vol. PS-8, No. 3, 1980, pp. 259–268.

[7]Miller, S. A., "Multifluid Nonequilibrium Simulations of Arcjet Thrusters," Ph.D. Dissertation, Massachusetts Inst. of Technology, Cambridge, MA, Feb. 1994.

[8]Pfender, E., "Electric Arcs and Arc Gas Heaters," *Gaseous Electronics*, edited by M. N. Hirsch and H. J. Oskam, Vol. 1, Academic, London, 1978.

[9]Jack, J. R., "Theoretical Performance of Propellants Suitable for Electrothermal Jet Engines," *ARS Journal*, Vol. 31, 1961, p. 1685.

[10]John, R. R., Bennett, S., Cass, L. A., Chen, M. M., and Connors, J. F., "Energy Addition and Loss Mechanisms in the Thermal Arcjet Engine," AIAA Paper 63-022, March 1963.

[11]Weber, H. E., "Growth of an Arc Column in Flow and Pressure Fields," AGARDoGraph 84, Sept. 1964, pp. 845–887.

[12]Topham, D. R., "The Electric Arc in a Constant Pressure Axial Gas Flow," *Journal of Physics D: Applied Physics*, Vol. 4, No. 7, 1971, pp. 1114–1125; also "Characteristics of Axial Flow Electric Arcs Subject to Pressure Gradients," *Journal of Physics D: Applied Physics*, Vol. 5, No. 1, 1972, pp. 533–541.

[13]Glocker, B., Schrade, H. O., and Sleziona, C., "Numerical Prediction of Arcjet Performance," AIAA Paper 90-2612, July 1990.

[14]Glocker, B., Schrade, H. O., and Auweter-Kurtz, M., "Performance Calculation of Arcjet Thrusters—The Three Channel Model," *Proceedings of the 23rd International Electric Propulsion Conference* (Seattle, WA), 1993 (Paper 93-187).

[15]Schrade, H. O., and Sleziona, P. C., "Performance Calculation of an H_2 Arcjet by Means of Dual Channel Model," *Proceedings of the 20th International Electric Propulsion Conference* (Garmish-Partenkirchen, Germany), 1988 (Paper 88-104).

[16]Martinez-Sanchez, M., and Sakamoto, A., "Simplified Analysis of Arcjet Thrusters," AIAA Paper 93-1904, June 1993.

[17]Tahara, H., Uda, N., Onoe, K., Tsubakishita, Y., and Yoshikawa, T., "Optical Measurement and Numerical Analysis of Medium-Power Arcjet Nonequilibrium Flowfields," *Proceedings of the 23rd International Electric Propulsion Conference* (Seattle, WA), 1993 (Paper 93-133).

[18]Tahara, H., Komiko, K., Zhang, L., and Onoe, K., "Plasma Features in a Medium Power Arcjet," *Proceedings of the 24th Electric Propulsion Conference* (Moscow), 1995 (Paper 95-16).

[19]Watson, V. R., and Pegot, E. B., "Numerical Calculations for the Characteristics of a Gas Flowing Axially Through a Constricted Arc," NASA TN D-4042, June 1967.

[20]Andrennucci, M., Scortecci, F., Capecci, G., and Wünsch, T., "Development of a Computer Programme for the Analysis of Arcjet Nozzles," *Proceedings of the 22nd International Electric Propulsion Conference* (Viareggio, Italy), 1991 (Paper 91-113).

[21]Nishida, M., Kaita, K., and Tanaka, K., "Numerical Studies of the Flow Field in a DC Arcjet Thruster," *Proceedings of the 20th International Electric Propulsion Conference* (Garmisch-Partenkirchen, Germany), 1988 (Paper 88-105).

[22]Tanaka, K., Tsuchiya, K., Kaita, K., and Nishida, M., "Computational Investigation on the Characteristics of a Low Power DC Arcjet Thruster," *Proceedings of the 23rd International Electric Propulsion Conference* (Garmisch Parten Kirchen, Germany), 1988 (Paper 88-106).

[23]Okamoto, H., and Nishida, M., "Numerical Simulation of the Performance of a Radiation-Cooled 1KW DC Arcjet Thruster," *Proceedings of the 23rd International Electric Propulsion Conference* (Seattle, WA), 1993 (Paper 93-181).

[24]Fujita, K., and Arakawa, Y., "Anode Heat Loss and Current Distributions in DC Arcjets," *Proceedings of the 23rd International Electric Propulsion Conference* (Seattle, WA), 1993 (Paper 93-185).

[25]Butler, G. W., Kashiwa, B. A., and King, D. Q., "Numerical Modeling of Arcjet Performance," AIAA Paper 90-1472, June 1990.

[26]Butler, G. W., and King, D. Q., "Single and Two-Fluid Simulations of Arcjet Performance," AIAA Paper 92-3104, 1992.

[27]Butler, G. W., Kull, A. E., and King, D. Q., "Single-Fluid Simulations of Low Power Hydrogen Arcjets," AIAA Paper 94-2870, June 1994.

[28]Rhodes, R., and Keefer, D., "Numerical Modeling of an Arcjet Thruster," AIAA Paper 90-2614, July 1990.

[29]Rhodes, R., and Keefer, D., "Comparison of Model Calculations with Experimental Data from Hydrogen Arcjets," *Proceedings of the 22nd International Electric Propulsion Conference* (Viareggio, Italy), 1991 (Paper 91-111).

[30]Rhodes, R., and Keefer, D., "Non-Equilibrium Modeling of Hydrogen Arcjet Thrusters," *Proceedings of the 23rd International Electric Propulsion Conference* (Seattle, WA), 1993 (Paper 93-217).

[31]Capelli, M. A., Liebeskind, J. G., Hanson, R. K., Butler, G. W., and King, D. Q., "A Direct Comparison of Hydrogen Arcjet Thruster Properties to Model Predictions," *Proceedings of the 23rd International Electric Propulsion Conference* (Seattle, WA), 1993 (Paper 93-220).

[32]Andrennucci, M., D'Agostino, L., and Ciucci, A., "Development of a Numerical Model of the Nozzle Flow in Low Power Arcjet Thrusters," *Proceedings of the 23rd International Electric Propulsion Conference* (Seattle, WA), 1993 (Paper 93-182).

[33]Capechi, G., and D'Agostino, L., "Numerical Model of Equilibrium Composition and Transport Coefficients of Hydrazine Under Dissociation and Ionization," AIAA Paper 94-2868, June 1994.

[34]Miller, S. A., and Martinez-Sanchez, M., "Two-Fluid Non-Equilibrium Simulation of Hydrogen Arcjet Thrusters," *Journal of Propulsion and Power*, Vol. 12, No. 1, 1996, pp. 112–119.

[35]Fujita, K., and Arakawa, Y., "Numerical Study of Non-Equilibrium Arcjet Constrictors Phenomena," 19th International Symposium on Space Technology and Science, Paper 94-a-52, Yokohama, Japan, 1994.

[36]Fujita, K., and Arakawa, Y., "Numerical Prediction of Arcjet Performance Based on the Chemical Kinetics and Electron Temperature Disparity," *Proceedings of the 24th International Electric Propulsion Conference* (Moscow), 1995 (Paper 95-25).

[37]Krier, H., Burton, R., and Megli, T., "Two-Temperature Modeling of N_2/H_2 Bipropellant Arcjets," AIAA Paper 94-2413, June 1994.

[38]Megli, T. W., Krier, H. J., and Burton, R. L., "A Plasmadynamic Model for Nonequilibrium Processes in N_2/H_2 Arcjets," AIAA Paper 95-1961, June 1995.

[39]Glocker, B., and Auweter-Kurtz, M., "Numerical and Experimental Constrictor Flow Analysis of a 10 kW Thermal Arcjet." AIAA Paper 92-3835, July 1992.

[40]Glocker, B., Roesgen, T., and Laxander, A., "Medium Power Arcjet Analysis and Experiments," *Proceedings of the 22nd International Electric Propulsion Conference* (Viareggio, Italy), 1991 (Paper 91-016).

[41]Sutton, G. W., and Sherman, A., *Engineering Magnetohydrodynamics*, McGraw–Hill, New York, 1965, p. 148, Fig. 5.6.

[42]Nighan, W. L., "Electron Energy Distributions and Collision Rates in Electrically Excited N_2, CO and CO_2," *Physical Review A: General Physics*, Vol. 2, No. 5, 1970, pp. 1989–2000.

[43]Maecker, H. H., "Principles of Arc Motion and Displacement," *Proceedings of the IEEE*, Vol. 59, No. 4, 1979, pp. 439–449.

[44]Yamada, T., Toki, K., and Kuriki, K., "Behavior of Arc Column in Arcjet Constrictor," *Proceedings of the 23rd International Electric Propulsion Conference* (Seattle, WA), 1993.

[45]Harris, W. J., O'Hair, E. A., Hatfield, L. L., Kristiansen, M., and Mankins, J. S., "Anode Motion in High Power Arcjets," AIAA Paper 92-3838, July 1992.

[46]Curran, F. M., and Sarmiento, C. J., "Low Power Arcjet Performance Characterization," AIAA Paper 90-2578, July 1990.

[47]Zube, D. M., and Myers, R. M., "Thermal Nonequilibrium in a Low Power Arcjet Nozzle," *Journal of Propulsion and Power*, Vol. 9, No. 4, 1993, pp. 545–552.

[48]Zube, D. M., and Auweter-Kurtz, M., "Spectroscopic Arcjet Diagnostic Under Thermal Equilibrium and Nonequilibrium Conditions," AIAA Paper 93-1792, June 1993.

[49]Park, C., "Hydrogen Line Ratios as Electron Temperature Indicators in Non-Equilibrium Plasma," *Journal of Quantitative Spectroscopy and Radioactive Transfer*, Vol. 12, No. 1, 1972, pp. 323–370.

[50]Hoskins, W. A., King, D. Q., and Butler, G. W., "Measurement of Population and Temperature Profiles in an Arcjet Plume," AIAA Paper 92-3240, July 1992.

[51]Fasoulas, S., Auweter-Kurtz, M., Habiger, H. A., Laure, S. H., and Sleziona, P. C., "Investigation of a Nitrogen Flow Within a Plasma Wind Tunnel," AIAA Paper 93-2817, July 1993.

[52]Capitelli, M. (ed.), *Nonequilibrium Vibrational Kinetics*, Springer–Verlag, Berlin, 1986.

[53]Babu, V., and Subramaniam, V., "2-D Axisymmetric Flow in Arcjets with Strong Vibrational Non-Equilibrium," *Proceedings of the 23rd International Electric Propulsion Conference* (Seattle, WA), 1993 (Paper 93-129).

[54]Gonzales, D. A., and Varghese, P. L., "Master Equation Calculations of Vibrational Non-Equilibrium and Dissociation Kinetics," International Union of Theoretical and Applied Mechanics Symposium, Marseille, France, Sept. 1992.

[55]Massey, H., and Craggs, J. D., *Handbuch der Physik*, 37/1, 1959, pp. 314–415.

[56]Mitchner, M., and Kruger, C. H., Jr., *Partially Ionized Gases*, Wiley-Interscience, New York, 1973, p. 107.

[57]Butler, G. W., and Cassady, R. J., "Directions for Arcjet Technology Development," *Journal of Propulsion and Power*, Vol. 12, No. 6, 1996, pp. 1026–1034.

[58]Auweter-Kurtz, M., Glocker, B., Kurtz, H. L., Loessener, O., Schrade, H. O., Turbanos, N., Wegmann, T., and Willer, D., "Cathode Phenomena in Plasma Thrusters," *Journal of Propulsion and Power*, Vol. 9, No. 56, 1993, pp. 882–888.